

# A Binuclear Iron(III) Schiff Base Complex Doubly Bridged by Hydroxyl Groups: Synthesis, Structure, and Characterization<sup>1</sup>

X. Feng<sup>a,\*</sup>, J. L. Chen<sup>b</sup>, G. Y. Luo<sup>a</sup>, L. Y. Wang<sup>a, b,\*</sup>, and J. Z. Guo<sup>a</sup>

<sup>a</sup> College of Chemistry and Chemical Engineering, Luoyang Normal University, Luoyang, 471022 P.R. China

<sup>b</sup> School of Life Science and Technology, Nanyang Normal University, Nanyang, 473061 P.R. China

\*e-mail: fengx@lynu.edu.cn

Received July 7, 2014

**Abstract**—A novel binuclear iron(III) Schiff base complex  $[\text{Fe}_2(\text{NO}_2\text{-Salpn})_2(\mu\text{-OH})_2] \cdot \text{H}_2\text{O}$  (**I**) ( $\text{NO}_2\text{-Salpn}$  = 5-nitrosalicylaldehyde-1,3-propanediamine) has been obtained through one-pot refluxing and condensation. Complex **I** was established by single-crystal X-ray diffraction analysis (CIF file CCDC no. 1005239) and further characterized by elemental analysis, IR spectroscopy, electrochemical and magnetochemical measurements. Complex **I** consists of two pseudo-octahedral high-spin iron(III) units doubly bridged by two hydroxyl groups. The inter hydrogen bonding interactions connect the adjacent binuclear units into one dimensional (1D) infinite chain, and these 1D chains are further propagated into the two dimensional (2D) supramolecular network by weak intermolecular interactions. Variable temperature magnetic measurements indicate the presence of strong antiferromagnetic interactions between the two adjacent iron(III) ions.

**DOI:** 10.1134/S1070328415020013

## INTRODUCTION

Recent years have witnessed that the ligand of salicylaldehyde Schiff base has elicited considerable attention due to the interests in the biology and chemistry fields, and many ligands of salicylaldehyde Schiff base have been documented [1–3]. Meanwhile, iron is an essential trace element, and is the main component of hemoglobin in human blood. Because the iron(III) ion has the most self-spin single electrons, the design, synthesis, and characterization of iron complexes with Schiff-base ligands play the vital role in coordination chemistry due to the importance as synthetic models for the functional materials [4–7]. In addition, as we all know, the pseudo-halide ions,  $\text{N}_3$  [8], diamine [9], and oxygen atom [10] have been well exploited for their ability to bridge paramagnetic moieties into dimers, clusters, and even polymers. However, the iron Schiff base complex incorporating electron-withdrawing groups, such as nitro group and neutral water bridge, are seldom reported, to the best of our knowledge [11, 12]. Hydroxyl group is one of the component substances of water, which is an important resource for the survival of all life on the plane, and the most important part of the organism. In this contribution, an unique binuclear iron complex based on substituted salicylaldehyde Schiff base ligand,  $[\text{Fe}_2(\text{NO}_2\text{-Salpn})_2(\mu\text{-OH})_2] \cdot \text{H}_2\text{O}$  (**I**), has been synthesized and characterized systematically, in which the two Fe-Schiff base moieties were doubly bridged by two hydroxyl moieties.

## EXPERIMENTAL

**Materials and physical measurements.** All reagents used in the syntheses were of analytical grade. Elemental analysis (C, H, and N) was performed on a PerkinElmer 2400 element analyzer. The infrared spectra ( $4000\text{--}650\text{ cm}^{-1}$ ) were recorded by using KBr pellet on a VECTRA-22 spectrometer. The variable temperature solid-state magnetic susceptibilities of title complex have been performed using a MPMS-7 SQUID magnetometer in the range 2–300 K at a magnetic field of 2000 Oe. Diamagnetic corrections were made with Pascal's constants for all constituent atoms. Electrochemical measurements were executed on RST3000 series electronic work station (Suzhou Risetech Instrument Co. Ltd., China). The electrochemical cell used in cyclic-voltammetry was a closed standard three-electrode cell connected to a solution reservoir through a Teflon tube under nitrogen atmosphere. A platinum disk (1.5 mm diameter) was used as the working electrode, and a  $\text{Hg}/\text{Hg}_2\text{Cl}_2$  as the reference electrode equipped with a wire counter electrode. The ferrocene/ferrocinium ( $\text{Fc}/\text{Fc}^+$ ) redox couple served as the internal standard.

**Synthesis of complex I.** The mixture of  $\text{Fe}(\text{NO}_3)_3 \cdot 9\text{H}_2\text{O}$  (80.799 mg, 0.2 mmol) and  $\text{KSCN}$  (38.872 mg, 0.2 mmol) was refluxed in anhydrous methanol (10 mL) at  $60^\circ\text{C}$  for 3 h in air, decanted off, and filtered. To the resulting red solution was added 10 mL DMF solution of freshly distilled 5-nitrosalicylaldehyde and 1,3-propanediamine at a molar ratio of 2 : 1 simultaneously. Then the solution was vigorously

<sup>1</sup> The article is published in the original.

**Table 1.** Crystallographic data and experimental details for complex **I**

Parameter	Value
Crystal shape/color	Block/red
Formula weight	460.70
Temperature, K	296(2)
Crystal system	Monoclinic
Space group	$P2_1/c$
Unit cell dimensions:	
$a$ , Å	11.633(3)
$b$ , Å	9.668(2)
$c$ , Å	16.799(4)
$\beta$ , deg	98.118(3)
$V$ , Å <sup>3</sup>	1870.4(7)
$Z$	4
$\rho_{\text{calcd}}$ , g cm <sup>-3</sup>	1.640
$F(000)$	950
Absorption coefficient, mm <sup>-1</sup>	0.863
$\theta$ Range for data collection, deg	2.44–25.50
Limiting indices ranges	$-14 \leq h \leq 14$ , $-11 \leq k \leq 11$ , $-20 \leq l \leq 20$
Reflections measured/independent	10716/3460
$R_{\text{int}}$	0.0350
Reflections with $I > 2\sigma(I)$	2423
Max and min transmissions	0.8532 and 0.7698
Data/restraints/parameters	3460/0/271
GOOF	1.013
$R$ indices ( $I > 2\sigma(I)$ )	$R_1 = 0.0381$ , $wR_2 = 0.0759$
$R$ indices (all data)	$R_1 = 0.0659$ , $wR_2 = 0.0895$
Largest diff. peak and hole, $e/\text{\AA}^3$	0.298 and $-0.317$

stirred for a further 2.5 h. After that, the mixture was cooled down to the room temperature naturally and filtered. One week later, dark red crystals were obtained and filtered. The yield was 0.038 g (41% based on Fe element).

For  $C_{17.50}N_4O_8Fe$

anal. calcd., %: C, 44.23; H, 3.80; N, 12.14; Fe, 12.10.

Found, %: C, 44.19; H, 3.74; N, 12.11; Fe, 12.04.

IR (KBr;  $\nu$ , cm<sup>-1</sup>): 3564 br, 1638 s, 1600 s, 1439 s, 1366 m, 1480 m, 874 m, 56 m.

**X-ray structure determination.** A single crystal of complex **I** ( $0.32 \times 0.21 \times 0.19$  mm) was mounted on a Bruker SMART APEX II CCD diffractometer equipped with a graphite-monochromatized  $MoK_{\alpha}$  radiation ( $\lambda = 0.71073$  Å) by using a  $\varphi/\omega$  scan mode at room temperature in the range of  $2.44^\circ \leq \theta \leq 25.50^\circ$ . Corrections for  $Lp$  factors were applied and all non-hydrogen atoms were refined with anisotropic thermal parameters. The structure was solved by direct methods with SHELXS-97 [13]. The hydrogen atoms were assigned with common isotropic displacement factors and included in the final refinement by use of geometrical restraints. A full-matrix least-squares refinement on  $F^2$  was carried out using SHELXL-97 [14]. The final  $R_1 = 0.0381$ ,  $wR_2 = 0.0759$  ( $w = 1/[\sigma^2(F_o^2) + (0.0220P^2) + 2.2693P]$ , where  $P = (F_o^2 + 2F_c^2)/3$ ),  $S = 1.013$ ,  $(\Delta\rho)_{\text{max}} = 0.298$  and  $(\Delta\rho)_{\text{mix}} = -0.317$  e/Å<sup>3</sup>. Crystallographic and experimental details are summarized in Table 1. The selected bond lengths and bond angles are listed in Table 2.

Supplementary material has been deposited with the Cambridge Crystallographic Data Centre (no. 1005239; deposit@ccdc.cam.ac.uk or <http://www.ccdc.cam.ac.uk>).

## RESULTS AND DISCUSSION

In IR spectrum of complex **I**, the presence of strong bands ranging from 1439 to 1600 cm<sup>-1</sup> indicates the existence of benzene ring. The broad band at  $\sim 3564$  cm<sup>-1</sup> is attributed to the free water molecule. Besides, the strong vibration peaks appear around 1638 cm<sup>-1</sup>, corresponding to the stretching vibrations of the C=N group. In addition, the absorption of 1366 to 1480 cm<sup>-1</sup> confirms the existence of nitro groups in complex **I**.

The X-ray diffraction analysis reveals that the title compound crystal structure consists of a Schiff base Fe complex and an uncoordinated water molecule. The perspective view of complex **I** with atom labeling scheme is illustrated in Fig. 1. In the Schiff base complex, there exist two  $[\text{Fe}(\text{NO}_2\text{-Salpn})]$  moieties and two coordinated water molecules, exhibiting the centrosymmetric configuration. The coordination environment around the  $\text{Fe}^{3+}$  ion can be described as a distorted octahedron. Each  $\text{Fe}^{3+}$  ion is six-coordinated by two N atoms of 1,3-propanediamine, two O atoms of 5-nitrosalicylaldehyde and two lattice water O atoms, which results in one fourmembered ring and three six-membered rings around the  $\text{Fe}^{3+}$  ion. The bond lengths of  $\text{Fe}(1)-\text{O}(2)$ ,  $\text{Fe}(1)-\text{O}(3)$ ,  $\text{Fe}(1)-\text{O}(4)$ ,  $\text{Fe}(1)-\text{N}(2)$  in equatorial plane are found to be 1.984, 1.946, 1.963, 2.133 Å, respectively; axial  $\text{Fe}(1)-\text{N}(1)$ ,  $\text{Fe}(1)-\text{O}(2)^{\#1}$  is 2.135, 1.993 Å, respectively. A slightly distorted octahedral geometry is also confirmed by the

**Table 2.** Selected bond lengths and angles for compound **I**

Bond	<i>d</i> , Å	Bond	<i>d</i> , Å	Bond	<i>d</i> , Å
Angle	$\omega$ , deg	Angle	$\omega$ , deg	Angle	$\omega$ , deg
Fe(1)–O(3)	1.946(2)	Fe(1)–O(2)	1.9843(19)	Fe(1)–N(2)	2.133(3)
Fe(1)–O(4)	1.963(2)	Fe(1)–O(2) <sup>#1</sup>	1.993(2)	Fe(1)–N(1)	2.135(2)
O(3)Fe(1)O(4)	91.63(9)	O(4)Fe(1)N(2)	167.34(9)	N(2)Fe(1)N(1)	83.32(10)
O(3)Fe(1)O(2)	92.13(9)	O(2)Fe(1)N(2)	95.40(9)	Fe(1)O(2)Fe(1) <sup>#1</sup>	105.03(9)
O(4)Fe(1)O(2)	96.78(9)	O(2) <sup>#1</sup> Fe(1)N(2)	91.84(9)	Fe(1)O(2)H(3w)	124.9
O(3)Fe(1)O(2) <sup>#1</sup>	166.22(8)	O(3)Fe(1)N(1)	101.92(10)	C(17)N(1)Fe(1)	118.3(2)
O(4)Fe(1)O(2) <sup>#1</sup>	94.62(9)	O(4)Fe(1)N(1)	85.71(9)	C(14)N(2)Fe(1)	122.9(2)
O(2)Fe(1)O(2) <sup>#1</sup>	74.97(9)	O(2)Fe(1)N(1)	165.68(9)	C(15)N(2)Fe(1)	118.5(2)
O(3)Fe(1)N(2)	84.48(10)	O(2) <sup>#1</sup> Fe(1)N(1)	90.79(9)	N(2)Fe(1)N(1)	83.32(10)

bond angles of O(2)Fe(1)O(2)<sup>#1</sup>, O(2)Fe(1)O(3), which are found to be 75.27(9) $^{\circ}$ , 91.99 $^{\circ}$ . Interestingly, Fe(NO<sub>2</sub>-Salen) moieties are bridged via two hydroxyl groups, and the Fe<sub>2</sub>O<sub>2</sub> core are completely coplanar. To the best of our knowledge, this is the first example that two adjacent iron(III) centers are bridged by hydroxyl group simultaneously based on substituted salicylaldehyde Schiff base ligand. However, in this case, the Fe···Fe separation in the Fe<sub>2</sub>O<sub>2</sub> core is mere 3.157 Å, which is seldom reported.

In our previous work, another dinuclear iron(III) analogous complex containing N,N-ethylene-bis(salicylideneiminato) monobridged via 4,4-bipyridine

had been synthesized, in which the distance between the two Fe atoms is 11.570 Å [15].

Close inspection reveals that there present obvious hydrogen bonding between the O(2) atom from coordinated water and O(7) of nitro group, and this hydrogen bonding connects the adjacent binuclear Schiff base complexes into 1D infinite chain, as displayed in Fig. 2. Hydrogen bond lengths and bond angles for complex **I** are listed in Table 3 for details. These 1D chains are further connected through the C–H···O bonds (C···O 3.511 Å) weak interaction, [16–18], which is between the C atoms of 5-nitrosalicylaldehyde and the oxygen atoms of uncoordinated waters, as well as the O–H···O bonds (O···O 3.049 Å) between

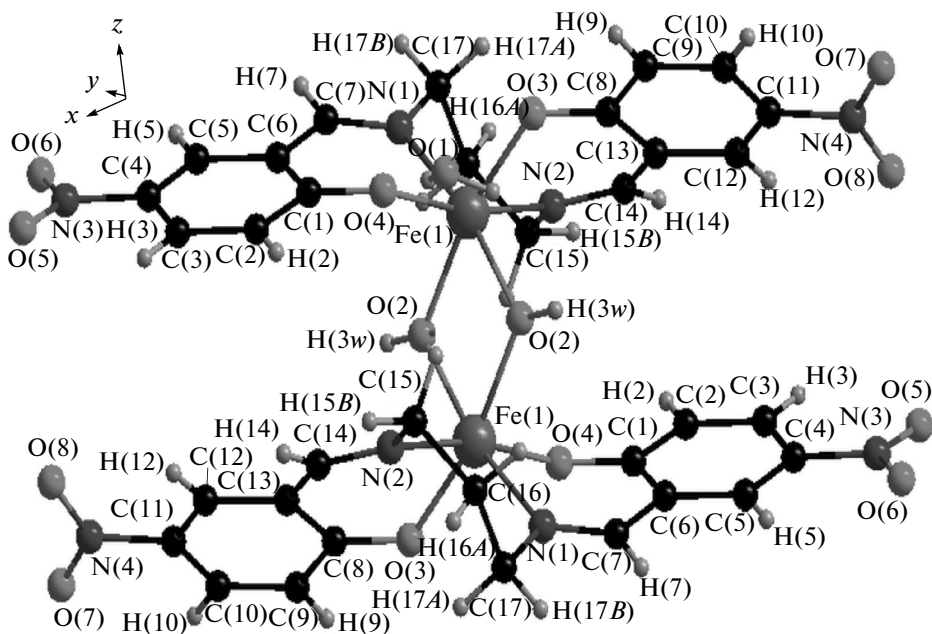


**Fig. 1.** Molecular structure of complex **I** with the atom-numbering scheme. The H atoms are illustrated as small spheres of arbitrary radii.

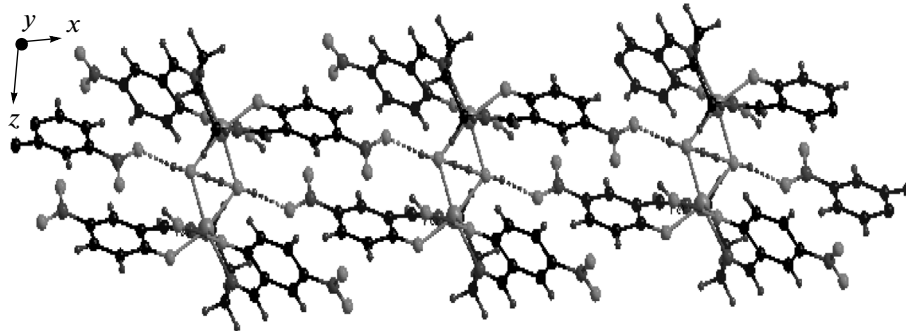


Fig. 2. Illustrating the 1D chain of complex I through hydrogen bonding.

the O atoms of 5-nitrosalicylaldehyde and the oxygen atoms of uncoordinated waters. It gives rise to the 2D supramolecular architecture as displayed in Fig. 3; the weak interactions above mentioned further cross linked these 2D sheets into final 3D structure as shown in Fig. 4.

The cyclic voltammogram of title complex was recorded at sweep rate of  $40 \text{ mV s}^{-1}$ , and the result is reported in Fig. 5a. The iron(III) complex exhibits a one-electron reduction process in the anodic potential of  $E_{\text{pa}} = -389 \text{ mV}$  and reduction peak potential of  $E_{\text{pc}} = -744 \text{ mV}$ , with  $i_{\text{pa}} = 0.51 \mu\text{A}$  and  $i_{\text{pc}} = 11.456 \mu\text{A}$ .  $\Delta E = |E_{\text{pa}} - E_{\text{pc}}| = 355 \text{ mV}$ , while  $i_{\text{pa}}/i_{\text{pc}} = 0.04$  and  $E_{1/2} = -566.5 \text{ mV}$ . The oxidation and reduction processes are irreversible in nature. When the scan rate was changed, the reduction peak potentials shift to the negative potential and the oxidation peak potentials shift to the positive potential very slightly as the scan rate increases, as illustrated in Fig. 5b.

The temperature dependence of the magnetic susceptibilities in the form of  $\chi_M T$  and  $\chi_M$  vs.  $T$  for title complex

Table 3. Geometric parameters of hydrogen bonds for complex I\*

D—H…A	Distance, Å			Angle DHA, deg
	D—H	H…A	D…A	
O(1)—H(1w)…O(8) <sup>#2</sup>	0.85	2.27	3.049(4)	153
O(1)—H(2w)…O(4)	0.85	2.13	2.982(3)	177
O(2)—H(3w)…O(7) <sup>#2</sup>	0.85	1.99	2.835(4)	170
O(2)—H(4w)…O(2) <sup>#1</sup>	0.85	1.58	2.434(4)	180

\* Symmetry codes: <sup>#1</sup>  $-x + 2, -y + 1, -z$ ; <sup>#2</sup>  $-x + 1, -y + 1, -z$ .

are given in Fig. 6. The  $\chi_M T$  value for compound I is  $2.69 \text{ cm}^3 \text{ K mol}^{-1}$  at room temperature, which is smaller than that of expected value for two uncoupled five independent spins  $S = 5/2$  ( $8.754 \text{ cm}^3 \text{ K mol}^{-1}$ ) of iron(III) [15]. Upon cooling the  $\chi_M T$  value decreases rapidly continuously to a value of  $0.07 \text{ cm}^3 \text{ K mol}^{-1}$  at 2 K. Such behavior can be referred to the presence of possible antiferromagnetically coupled interactions between the two iron atoms. There are two pathways of magnetic interaction in the present system, namely, (i) the short distance between the two Fe(III) atoms in complex I; (ii) the complete coplanar  $\text{Fe}_2\text{O}_2$  rhomb core.

In order to quantitatively understand the magnitude of the spin-exchange interaction, for similar dinuclear iron(III) complexes, the following Eq. (1) is induced from the spin Hamiltonian  $\hat{H} = -J\hat{S}_1\hat{S}_2$ , typically  $J$  is determined from a fitting of the magnetic susceptibility data using the Van Vleck equation evaluated for an exchange-coupled high-spin dinuclear Fe(III) complex [19, 20]:

$$\chi_M = \frac{Ng^2\beta^2}{4KT} \left[ \frac{A}{B} \right], \quad (1)$$

$$A = 8(e^x + 5e^{3x} + 14e^{6x} + 30e^{10x} + 55e^{15x}),$$

$$B = (1 + 3e^x + 5e^{3x} + 7e^{6x} + 9e^{10x} + 11e^{15x}),$$

where  $\chi = |J|/KT$ . An additional coupling parameter ( $zJ'$ ), was added in Eq. (2) to take into account the magnetic behavior between the 1D chains as a molecular field approximation [21]

$$\chi_M = \frac{\chi_{bi}}{1 - \frac{2zJ'}{N\beta^2 g^2} \chi_{bi}}. \quad (2)$$

The least-squares analysis of magnetic susceptibilities data led to  $J = -9.9909 \text{ cm}^{-1}$ ,  $g = 1.8691$ , and  $R = 0.759 \times 10^{-3}$  (the agreement factor defined as

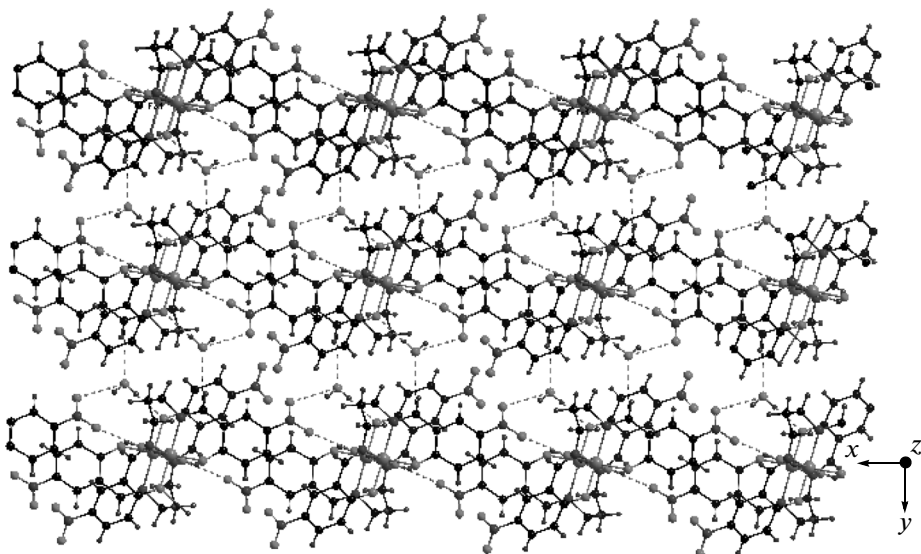


Fig. 3. The schematic diagram of 2D layer in complex I approximately along  $z$  axis.

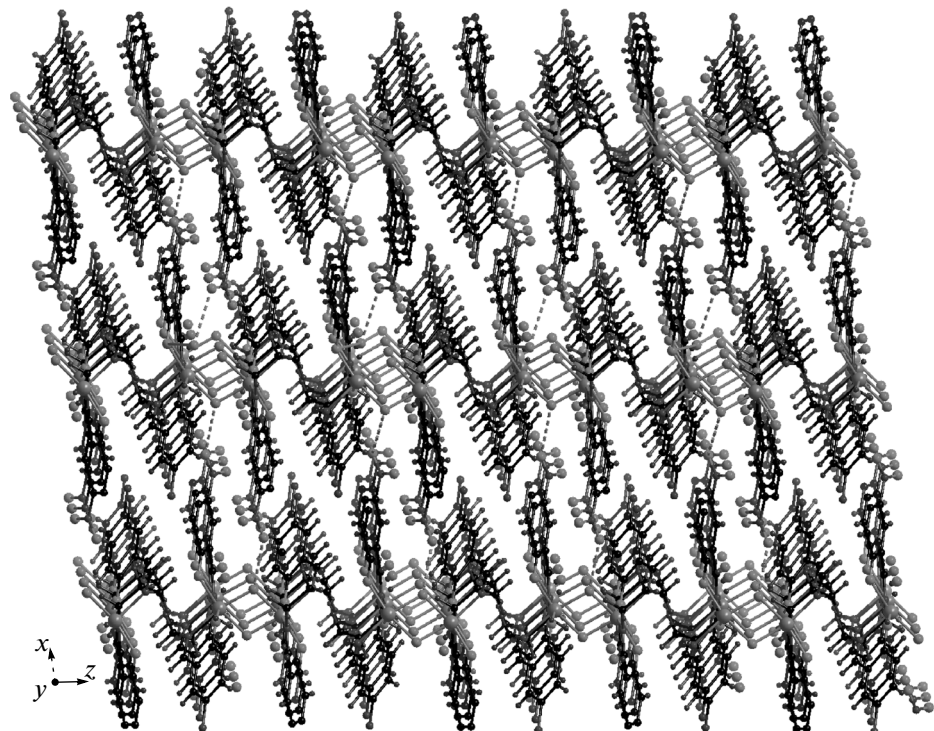
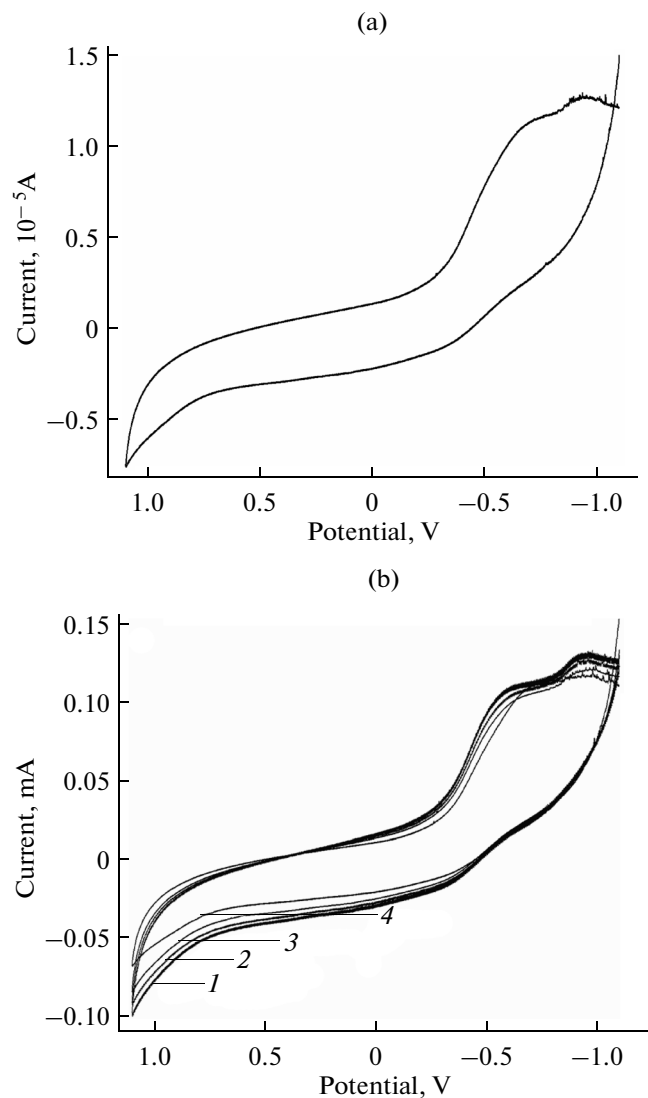


Fig. 4. The schematic diagram of 3D layer in complex I approximately along the  $y$  axis.

$R = \sum[(\chi_M)_{\text{obs}} - (\chi_M)_{\text{calc}}]^2 / \sum[(\chi_M)_{\text{obs}}]^2$ . The  $J$  value indicates a strong antiferromagnetic interaction between the two  $\text{Fe}^{3+}$  ions bridged by water molecules.

The strong antiferromagnetic exchange coupling is principally attributed to two factors: (i) the adjacent

two iron(III) ions bridged by water molecule, in which the two Fe atoms and two O atoms of the two coordinated water molecules are completely coplanar. In this complex, the Fe–Fe separation is 3.157 Å, and the  $\text{FeOFe}$  angle is 104.73°, which are comparable with



**Fig. 5.** Cyclic voltammogram of complex **I** at sweep rate  $40 \text{ mV s}^{-1}$  (a) and at sweep rates: 50 (1), 80 (2), 100 (3) and  $200 \text{ mV s}^{-1}$  (4) (b).

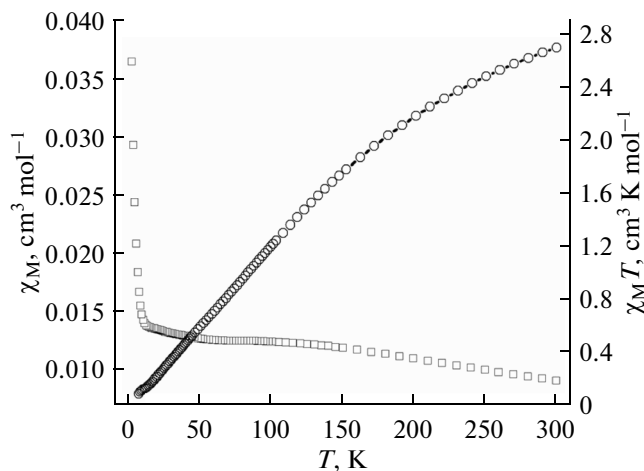


**Fig. 6.** Variable-temperature magnetic susceptibility data for complex **I**. The rectangles (□) represent the experimental data for the molar susceptibility ( $\chi_M$ ) and circles (○) represent the  $\chi_M T$ .

those reported previously in double-bridged diiron complexes [22–25] (the previous studies are listed in Table 4); (ii) the four atoms of the  $\text{Fe}_2\text{O}_2$  rohmb core are complete coplanar.

#### ACKNOWLEDGMENTS

This work was supported by the National Natural Science Foundation of China (no. 21273101 and 21271098), Program for Science & Technology Innovation Talents in Universities of Henan Province (2014HASTIT014), and Tackle Key Problem of Science and Technology Project of Henan Province, China (no. 142102310483), and Program for University of Malaya (UM.C/625/1/HIR/247).

**Table 4.** Parameters list about analogous oxygen double-bridged biiron complexes

Complex	Bridging	Fe–Fe, Å	FeOFe angle, deg	$J, \text{cm}^{-1}$	Reference
$[\text{Fe}_2(\text{O})_2(6\text{-Me}_3\text{-TPA})_2](\text{ClO}_4)_2$	$\mu\text{-O}$	2.71	92.5(2)	54(8)	22
$[\text{Fe}_2(\text{O})(\text{OH})(\text{BPEEN})_2](\text{ClO}_4)_3$	$\mu\text{-O}$	2.84		106(10)	22
$\text{C}_{24}\text{H}_{36}\text{N}_{10}\text{O}_4\text{Fe}_2$	$\mu\text{-OMe}$	3.220(1)	105.77(6)		23
$\text{C}_{20}\text{H}_{28}\text{N}_{10}\text{O}_4\text{Fe}_2 \cdot \text{H}_2\text{O}$ (2a)	$\mu\text{-OH}$	3.135(1)	104.56(16)		23
$\text{C}_{20}\text{H}_{28}\text{N}_{10}\text{O}_4\text{Fe}_2 \cdot \text{H}_2\text{O}$ (2b)	$\mu\text{-OH}$	3.084(1)	102.55(15)		23
$\text{C}_{28}\text{H}_{32}\text{N}_{10}\text{O}_{14}\text{Fe}_2$	O	3.208	107.77(8)		24
$\text{C}_{42}\text{H}_{48}\text{N}_6\text{O}_8\text{Fe}_2$	O	3.133	76.43(8)		24
$\text{C}_{40}\text{H}_{40}\text{N}_4\text{O}_8\text{Fe}_2$	$\text{C}_2\text{O}_4$	5.538		-3.89	24
$\text{C}_{38}\text{H}_{32}\text{N}_8\text{O}_4\text{Cl}_2\text{Fe}_2 \cdot \text{CH}_4\text{O}$ (a)	$\mu\text{-OMe}$	3.1465(10)	104.52(11)	-41.6	25
$\text{C}_{38}\text{H}_{32}\text{N}_8\text{O}_4\text{Cl}_2\text{Fe}_2 \cdot \text{CH}_4\text{O}$ (b)	$\mu\text{-OMe}$	3.1863(10)	105.27(11)	-44.7	25
This case	$\text{H}_2\text{O}$	3.157	104.73		

## REFERENCES

1. Savalia, R.V., Patel, A.P., Trivedi, P.T., et al., *Res. J. Chem. Sci.*, 2013, vol. 1, p. 97.
2. Feng, X., Xie, C.Z., Wang, L.Y., et al., *J. Chem. Crystallogr.*, 2008, vol. 38, p. 619.
3. Naiya, S., Biswas, S., Drew, M.G.B., et al., *Inorg. Chem.*, 2012, vol. 51, no. 9, p. 5332.
4. Kannappan, R., Tanase, S., Mutikainen, U.I., and Reedijk, T.J., *Polyhedron*, 2006, vol. 251, p. 646.
5. Vilalta, C.C., Rumberger, E., Brechin, E.K., et al., *Dalton Trans.*, 2002, no. 10, p. 4005.
6. Glaser, T., Pawelke, R.H., and Heidemeier, M., *Z. Anorg. Allg. Chem.*, 2003, vol. 629, no. 12, p. 2274.
7. Sivasubramanian, V.K., Ganesan, M., and Rajagopal, S., *J. Org. Chem.*, 2002, vol. 67, no. 5, p. 1506.
8. Reddy, K.R., Rajasekharan, M.V., and Tuchagues, J.P., *Inorg. Chem.*, 1998, vol. 37, no. 22, p. 5978.
9. Feng, X., Li, S.H., Sun, Q.Q., et al., *Russ. J. Coord. Chem.*, 2011, vol. 37, no. 5, p. 377.
10. Zheng, H., Zang, Y., Dong, Y.H., et al., *J. Am. Chem. Soc.*, 1999, vol. 121, no. 10, p. 2226.
11. Qian, S.S., Li, H.H., Zhu, H., et al., *Synth. React. Inorg., Met.-Org., Nano-Met. Chem.*, 2013, vol. 43, no. 4, p. 412.
12. Feng, X., Song, H.L., Ye, B.X., et al., *Chin. J. Struct. Chem.*, 2014, vol. 33, no. 6, p. 897.
13. Sheldrick, G.M., *SHELXS-97, Program for the Solution of Crystal Structure*, Göttingen: Univ. of Göttingen, 1997.
14. Sheldrick, G.M., *SHELXL-97, Program for the Crystal Structure Refinement*, Göttingen: Univ. of Göttingen, 1997.
15. Feng, X., Wang, J.G., Xie, C.Z., and Ma, N., *Z. Anorg. Allg. Chem.*, 2007, vol. 633, no. 12, p. 2085.
16. Zierke, M., Smiesko, M., Rabbani, S., et al., *J. Am. Chem. Soc.* 2013, vol. 135, no. 36, p. 13464.
17. Granijo, J., Gaviño, R., Freire, E., and Baggio R., *J. Mol. Struct.*, 2014, vol. 1063, no. 4, p. 102.
18. Ahmad, I., Pathak, V., Vasudev, P.G., et al., *RSC Adv.*, 2014, vol. 4, p. 24619.
19. Tanase, S., Bouwman, E., Bouwman, G.J., et al., *Polyhedron*, 2005, vol. 24, no. 1, p. 41.
20. Kahn, O., *Molecular Magnetism*, New York: Wiley-VCH, 1993.
21. O'Connor, C.J., *Prog Inorg. Chem.*, 1982, vol. 29, p. 203.
22. Naiya, S., Giri, S., Biswas, S., et al., *Polyhedron*, 2014, vol. 73, p. 139.
23. Li, F., Wang, M., Li, P., et al., *Inorg. Chem.*, 2007, vol. 46, no. 22, p. 9364.
24. Jia, H.P., Li, W., Ju, Z.F., and Zhang, J., *J. Mol. Struct.*, 2007, vol. 833, no. 1, p. 49.
25. Bikas, R., Monfared, H.H., Zoppellaro, G., et al., *Dalton Trans.*, 2013, vol. 42, p. 2803.